

Using Surrogate Meteorological Data to Predict the Hydrology of a Water Balance Cover

Christopher A. Bareither¹; Joy C. Foley²; and Craig H. Benson³

Abstract: The objective of this study was to evaluate strategies for addressing missing meteorological (MET) data when predicting the hydrology of a water balance cover for a waste-containment system using a variably-saturated flow code. Predicting the hydrology of water balance covers typically requires site-specific daily MET data, which may be only partially available (e.g., dew point temperature (T_{dew}), solar radiation (R_s), wind speed, and cloud cover frequently are only partly available). Thus, some of the input data may need to be estimated or surrogate data employed for hydrologic modeling. The influence of replacing missing MET data with estimates on hydrologic predictions was evaluated for a water balance cover in a semiarid climate. Substitution of single or multiple MET variables with long-term averages led to statistically similar predictions of annual percolation relative to percolation predicted using actual data. Replacing all MET variables (T_{dew} , R_s , wind speed, and cloud cover) with long-term averages underpredicted percolation by 25% (0.58 mm/year), on average, relative to percolation predicted with actual data. A strategy for estimating MET data via empirical techniques is described that includes estimating (1) T_{dew} = daily minimum temperature, (2) R_s with the Hargreaves and Samani model, (3) daily wind speed set equal to monthly averages, and (4) cloud cover estimated as a function of solar radiation. This surrogate MET data technique yielded modest overpredictions of annual percolation of 3 and 46% (0.07 and 1.08 mm/year) that were statistically similar to percolation predicted using actual data. DOI: 10.1061/(ASCE)GT.1943-5606.0001437. © 2015 American Society of Civil Engineers.

Author keywords: Hydrologic modeling; Landfill; Meteorological data; Unsaturated soil; Waste containment; Water balance covers.

Introduction

Earthen final covers for waste containment where soil water storage and evapotranspiration are used to control the percolation rate [so called water balance covers or evapotranspirative covers, (Albright et al. 2010)] are designed using principles of variably saturated flow (Khire et al. 2000; Albright et al. 2004, 2010; Malusis and Benson 2006; Apiwantragoon et al. 2014). Water balance covers provide an alternative to conventional covers employing hydraulic barrier layers (e.g., compacted clay layers, geomembranes, geosynthetic clay liners, and/or combinations thereof) for long-term isolation of waste and can be used to control percolation to minute amounts in arid and semiarid environments where precipitation is favorably balanced by energy available for evaporation and transpiration (Albright et al. 2004, 2013; Apiwantragoon et al. 2014). Monolithic and capillary barriers are the most common forms of water balance covers (Nyhan et al. 1997; Zornberg et al. 2003, Benson 2001; Scanlon et al. 2005; Ogorzalek et al. 2007; Zornberg

and McCartney 2007; Bohnhoff et al. 2009; Tallon et al. 2011; Apiwantragoon et al. 2014). Both types of covers employ a fine-textured soil layer (a storage layer) with adequate moisture-retention capacity to store infiltrating water during wetter periods, which subsequently is removed and returned to the atmosphere via evapotranspiration (ET) during drier periods. Capillary barriers include at least one clean coarse-grained soil layer below the fine-textured soil to provide a contrast in unsaturated hydraulic properties that enhances water-storage capacity of the storage layer and in some cases is used to promote lateral diversion of unsaturated flow (Stormont and Morris 1998; Khire et al. 2000).

Adoption of a water balance cover in lieu of a conventional cover for waste containment typically requires that the water balance cover have equivalent or superior ability to limit percolation through the cover system relative to a prescribed conventional cover, or that percolation fall below a prescribed threshold (Albright et al. 2010). Water balance modeling using variably-saturated flow codes generally is a key step, amongst other analyses, in demonstrating an equivalent or acceptable percolation rate (Benson and Bareither 2012).

Water balance modeling for a given cover profile requires definition of soil hydraulic properties, vegetation characteristics defining phenology and root water uptake, and meteorological (MET) data representative of a climatic period of interest (e.g., typical precipitation year or wettest year on record). Daily measurements of maximum and minimum air temperature (T_{max} and T_{min}), precipitation, dew point temperature (T_{dew}), solar radiation (R_s), wind speed, and cloud cover generally are required in the MET data set. Model simulations that may be required for water balance evaluations include a typical year of precipitation, wettest precipitation year on record, a year representing the 95th percentile of the wettest year on record, or a series of adjacent years (e.g., 5–10 years) that represent the highest precipitation period on record (Albright et al. 2010; Benson and Bareither 2012).

¹Assistant Professor, Dept. of Civil and Environmental Engineering, Colorado State Univ., Fort Collins, CO 80523 (corresponding author). E-mail: christopher.bareither@colostate.edu

²Graduate Research Assistant, Dept. of Civil and Environmental Engineering, Colorado School of Mines, Golden, CO 80401; formerly, Undergraduate Research Assistant, Civil and Environmental Engineering, Colorado State Univ., Fort Collins, CO 80523. E-mail: joycofoley@gmail.com

³Dean, School of Engineering and Applied Science, Hamilton Professor, Civil and Environmental Engineering, Univ. of Virginia, Charlottesville, VA 22904; formerly, Wisconsin Distinguished Professor and Chair, Geological Engineering, Univ. of Wisconsin-Madison, Madison, WI 53706. E-mail: chbenson@wisc.edu; chbenson@virginia.edu

Note. This manuscript was submitted on January 20, 2015; approved on September 23, 2015; published online on December 8, 2015. Discussion period open until May 8, 2016; separate discussions must be submitted for individual papers. This paper is part of the *Journal of Geotechnical and Geoenvironmental Engineering*, © ASCE, ISSN 1090-0241.

Identifying actual calendar years that represent these different hydrologic scenarios requires historical daily precipitation records, which generally are available along with T_{\max} and T_{\min} . However, compiling the entire MET data set required for water balance modeling (i.e., T_{dew} , R_s , wind speed, and cloud cover) can be difficult and may not be possible for a given site depending on the calendar year required for modeling or geographic location of the site. In such cases, design engineers must use surrogate data (e.g., estimates, approximates, or substituted data), but often are challenged regarding the impact that surrogate data have on hydrologic predictions. Previous parametric studies on hydrologic modeling of water balance covers have focused on the effects of cover thickness, soil properties, vegetation characteristics, and precipitation on hydrologic behavior (Zornberg et al. 2003; Zhang and Sun 2014). This study is constructed to aid practicing engineers who often are challenged with demonstrating equivalency of a water balance cover design to a conventional cover, but may not have access to all MET data to complete the necessary hydrologic modeling.

The objective of this study was to evaluate how replacing missing MET data with surrogates affected hydrologic predictions for a water balance cover located at a disposal site in semiarid Missoula, Montana (Benson and Bareither 2012). Numerical modeling was conducted using the code *WinUNSAT-H*, which simulates variably saturated flow, root water uptake, and climatic interaction (Benson 2007, 2010; Ogorzalek et al. 2007; Bohnhoff et al. 2009). *WinUNSAT-H* is an implementation of the *UNSAT-H* variably-saturated flow code developed at Pacific Northwest National Laboratory (Fayer 2000) for use in the Microsoft Windows operating system. *UNSAT-H* was developed by Pacific Northwest National Laboratory (Richland, Washington) for evaluating near surface hydrology of earthen covers and other ground surfaces at the U.S. Department of Energy's Hanford site. Hydrologic simulations were conducted using a complete data set comprised of daily MET data for a 20-year period (1991–2010). Comparative simulations were then conducted using surrogate data for T_{dew} , R_s , wind speed, and/or cloud cover. Differences between predictions made with the complete data set and data sets with surrogates were identified to understand the impact of surrogate data on hydrological predictions. Emphasis was placed on the prediction of percolation, which is the variable of greatest importance in practice when designing and permitting a water balance cover. Recommendations to address missing data in the MET data set are made based on outcomes of the comparative simulations.

Water Balance Modeling

The variably saturated flow model *WinUNSAT-H* (and DOS counterpart *UNSAT-H*, Fayer 2000) is a widely-used numerical model for simulating hydrologic behavior of water balance covers (Benson 2007). When properly parameterized, *WinUNSAT-H* yields reliable predictions of the hydrology of water balance covers, and overpredicts percolation modestly in most cases (Khire et al. 1997; Scanlon et al. 2005; Ogorzalek et al. 2007; Bohnhoff et al. 2009).

A detailed description of *UNSAT-H* can be found in Fayer (2000) and an overview of the model is presented in Khire et al. (1997, 2000), Ogorzalek et al. (2007), and Bohnhoff et al. (2009). In brief, *UNSAT-H* is a one-dimensional finite-difference computer program for simulating water and heat flow in unsaturated soil that solves a modified-Richards' partial differential equation for liquid and vapor water flow. The modified-Richards' equation that is solved is

$$\frac{\partial \theta}{\partial \psi} \frac{\partial \psi}{\partial t} = - \frac{\partial}{\partial z} \left(K_T \frac{\partial \psi}{\partial z} + K_u + q_{vT} \right) - S(z, t) \quad (1)$$

where θ = volumetric water content; ψ = matric suction; t = time; z = vertical coordinate; K_u = unsaturated hydraulic conductivity; $K_T = K_u + K_{v\psi}$, where $K_{v\psi}$ = isothermal vapor conductivity, q_{vT} = thermal vapor flux density, and $S(z, t)$ = sink term representing water uptake by vegetation. The thermal vapor flux density (q_{vT}) is computed using Fick's law of vapor diffusion. All simulations conducted in this study assumed isothermal conditions within the domain.

The sink term in Eq. (1), S , is for root water uptake, which is simulated by applying the transpiration demand amongst nodes in the root zone in proportion to the root density profile. Potential transpiration demand is determined by separating potential evapotranspiration (ET_p) into potential evaporation (E_p) and potential transpiration (T_p) as a function of leaf-area index (LAI) via the formulation by Ritchie and Burnett (1971). Actual transpiration demand at each node is set as a fraction of the applied potential transpiration demand depending on the water status in the root zone (Fayer and Jones 1990) using the Feddes et al. (1978) water stress function. Actual transpiration is set to zero if anoxic conditions exist (i.e., suction is less than the anaerobiosis point, ψ_a , which is near saturation) or if the suction exceeds the wilting point (ψ_{wp}). For suctions between the wilting point and the limiting point (ψ_l), the applied transpiration demand is assumed to vary linearly between zero and the potential transpiration.

Potential evapotranspiration in *WinUNSAT-H* is computed using the following form of the Penman equation (Penman 1948):

$$ET_p = \left(\frac{\Delta \cdot R_n}{\Delta + \gamma} \right) + \left\{ \left(\frac{\gamma}{\Delta + \gamma} \right) \left[0.27 \left(1 + \frac{U}{100} \right) \right] (e_a - e_d) \right\} \quad (2)$$

where Δ = slope (i.e., rate change) in the saturation vapor pressure-temperature curve; γ = psychrometric constant; R_n = net solar radiation expressed in equivalent evaporation; U = average 24-h wind speed measured at 2-m above the ground surface; e_a = saturation vapor pressure at mean air temperature; and e_d = actual vapor pressure. All MET data required for water balance modeling in *WinUNSAT-H*, with the exception of precipitation, are used to compute ET_p . Additional details on the Penman equation and calculations for ET_p can be found in Doorenbos and Pruitt (1977), Campbell and Norman (1998), and Fayer (2000).

Net solar radiation (R_n) is computed as function of global solar radiation (R_s), surface albedo (α), and net longwave radiation (R_{nL}). Global solar radiation is required input data for *WinUNSAT-H*, R_{nL} is computed within the program as a function of air temperature, vapor pressure, and cloud cover, and α was assumed equal to 0.25 for all simulations to represent established vegetation (Roessler et al. 2002). Calculations of e_a , e_d , and Δ in Eq. (2) are a function of saturation vapor pressure and air temperature, whereby the arithmetic average of T_{\max} and T_{\min} is used to compute e_a and T_{dew} is used to compute e_d .

Solar radiation, cloud cover, and T_{dew} affect the first term on the right-hand side of Eq. (2), which is referred to as the radiation term. As measured solar radiation at Earth's surface, R_s , increases, R_n in Eq. (2) increases and ET_p increases. As cloud cover and T_{dew} increase, there is an increase in atmospheric density due to increased abundance of atmospheric moisture, which contributes to decreasing ET_p . The second term on the right-hand side of Eq. (2) is referred to as the aerodynamic term and includes effects of wind speed and air temperature (T_{\max} , T_{\min} , and T_{dew}). As wind speed increases, the entire aerodynamic term increases, which causes ET_p to increase. A decrease in T_{dew} decreases e_d and results in

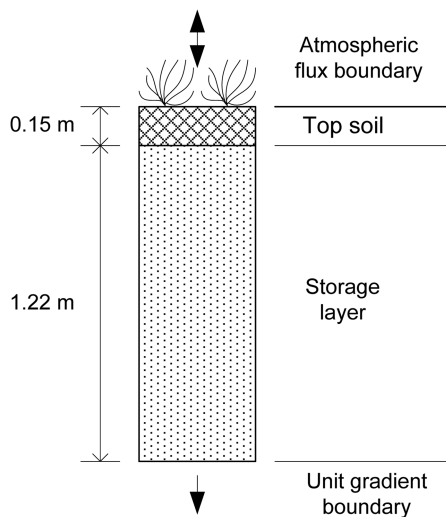


Fig. 1. Water balance cover profile and top and bottom boundary conditions used in the water balance models

a greater saturation vapor pressure deficit ($e_a - e_d$). Thus, a decrease in T_{dew} will increase ET_p . The maximum and minimum air temperatures also affect the aerodynamic and radiation terms in Eq. (1) via Δ and e_a ; however, in this study T_{max} and T_{min} were assumed known and their influence on ET_p were not directly evaluated.

Site Description

The modeling in this study was conducted to support the design and permitting of a water balance cover for a municipal solid waste landfill in Missoula, Montana. The cover employs a monolithic design comprised of a 1.22-m-thick storage layer overlain by a 0.15-m-thick topsoil layer (Fig. 1). Soil and vegetation characteristics used for water balance modeling were obtained from site-specific measurements reported in Benson and Bareither (2012). A detailed discussion of this site along with the soil properties and vegetation parameters needed for water balance modeling can be found in Benson and Bareither (2012).

Soil Properties

Characteristics of the soil layers used in the water balance models are summarized in Table 1 with the hydraulic properties shown in Figs. 2(a and c). The soil-water characteristic curve for each soil [Fig. 2(a)] was described by the following form of the van Genuchten function (van Genuchten 1980):

$$\Theta = \frac{\theta - \theta_r}{\theta_s - \theta_r} = \left[\frac{1}{1 + (\alpha \cdot \psi)^n} \right]^{1-n^{-1}} \quad (3)$$

where Θ = effective saturation; θ_s = saturated volumetric water content; θ_r = residual volumetric water content; and α and n = shape

Table 1. Characteristics of Soil Layers Used in Water Balance Modeling

Site	Soil ^a	Thickness (m)	Hydraulic properties				
			K_s (cm/s)	α (kPa ⁻¹)	n	θ_s	θ_r
Topsoil	SM	0.15	2.8×10^{-5}	0.050	1.33	0.50	0.00
Storage layer	SM	1.22	6.0×10^{-4}	0.145	1.27	0.35	0.00

Note: K_s = saturated hydraulic conductivity; α and n = fitting parameters for van Genuchten (1980) equation; θ_s = saturated volumetric water content; θ_r = residual volumetric water content.

^aUnified soil classification system, ASTM D2487 (ASTM 2011).

parameters. The unsaturated hydraulic conductivity (K_u) corresponding to water content θ was described using the van Genuchten-Mualem function (van Genuchten 1980)

$$K_u = K_s \cdot \Theta^\ell [1 - (1 - \Theta^{1/m})^m]^2 \quad (4)$$

where K_s = saturated hydraulic conductivity; and ℓ = pore interaction term, which was assumed equal to -2 for all simulations (Schaap and Leij 2000). Hysteresis in unsaturated hydraulic properties was not considered.

The measured K_s of the topsoil and storage layers were increased one order of magnitude [Fig. 2(c)] to account for pedogenesis and to limit runoff as recommended in Albright et al. (2010). This adjusted K_s also ensured that percolation would not be underpredicted.

Vegetation

Vegetation characteristics input to *WinUNSAT-H* included the temporal distribution of *LAI*, the root density profile, and water stress parameters for the transpiration function. Surface biomass samples were collected to measure *LAI*, and soil samples were collected in 150-mm intervals along the sidewall of a vertical pit to assess root density (Benson and Bareither 2012) using the Weaver-Darland method (Böhm 1979).

Root length densities (R_d), as described in Benson and Bareither (2012), were represented by

$$R_d = a \cdot e^{-z \cdot b} + c \quad (5)$$

where z = depth (m); and a , b , and c = empirical shape parameters [Fig. 2(b)]. The *LAI* was assumed to follow the trapezoidal function described in Albright et al. (2010), increasing linearly from 0 on Julian Day 130 to 1.42 on Julian Day 160, remaining constant at 1.42 until Julian Day 271, and then decreasing linearly to 0 on Julian Day 301 [Fig. 2(d)]. The wilting point was set at 3,532 kPa, the anaerobiosis point at 32 kPa, and the limiting point at 146 kPa based on recommended parameters for a site with similar vegetation and climate in Polson, Montana (Roesler et al. 2002; Benson and Bareither 2012). The maximum root depth was set at the base of the cover profile and the root growth rate was set at 3 mm/day (Roesler et al. 2002).

Meteorological Data

The 20-year time period spanning 1991–2010 was selected for the simulations in this study. This selection was based on the availability of a complete daily MET data set for all required input parameters: (1) T_{max} and T_{min} , (2) precipitation, (3) T_{dew} , (4) R_s , (5) wind speed, and (6) cloud cover. A compilation of MET data resources accessed by the authors is in Table 2. For this study, T_{max} and T_{min} , precipitation, and T_{dew} were obtained from the National Climate Data Center, whereas R_s , wind speed, and cloud cover were obtained from the National Solar Radiation Database. These two resources, along with the Western Regional Climate Center (Reno, Nevada), are recommended resources for accessing MET data for water balance modeling.

Solar radiation data compiled by the National Solar Radiation Database include measured data for select locations and modeled data for the majority of locations. Modeled data are based on three available models that have all been shown to yield comparable predictions of measured R_s (Wilcox 2012). Solar radiation data used in this study were from the METSTAT model developed by the National Renewable Energy Laboratory. This model was selected based on availability of R_s for the time period analyzed (i.e., 1991–2010).

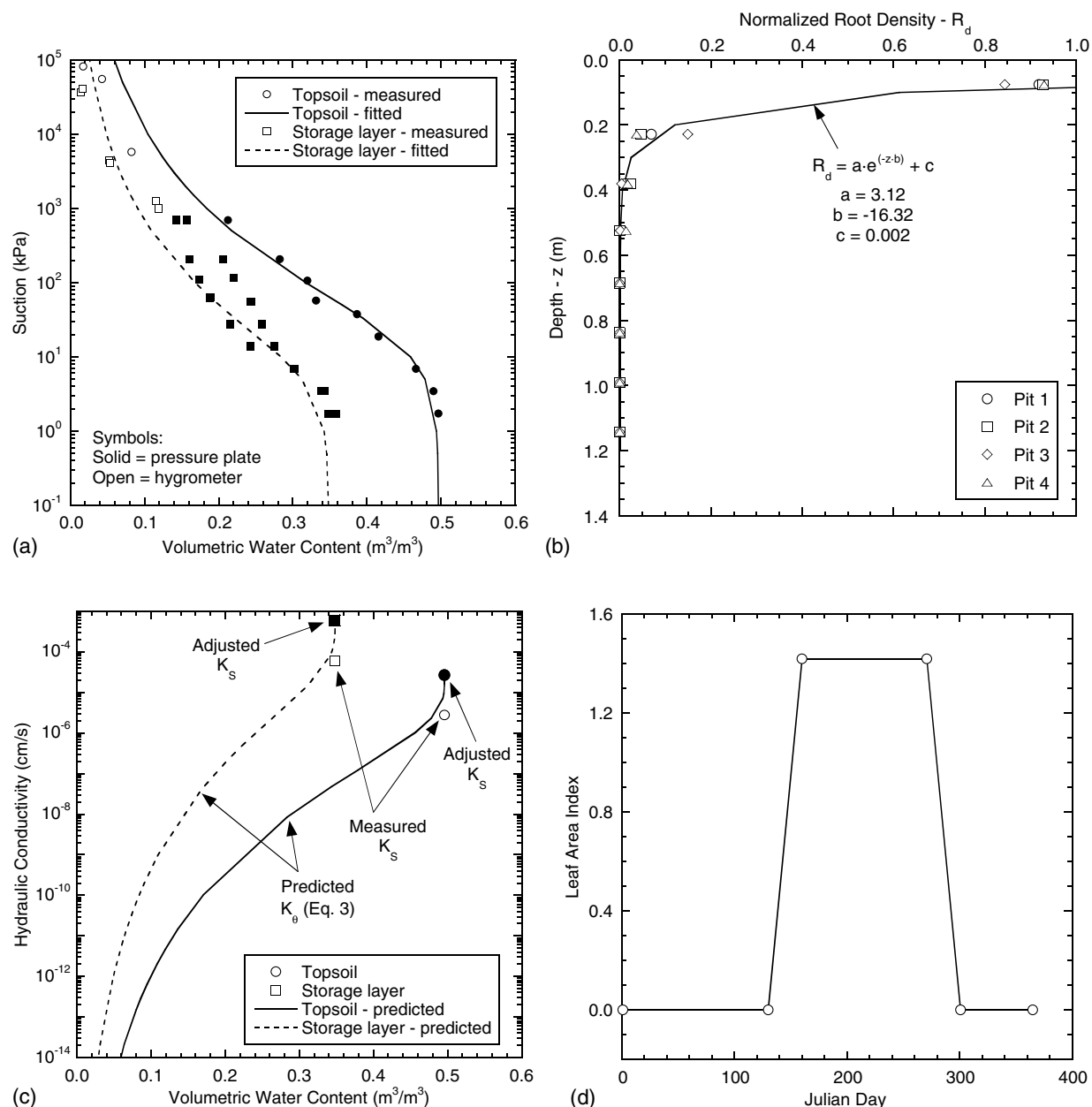


Fig. 2. Soil and vegetation characteristic relationships for the cover system profile: (a) soil suction versus volumetric water content for the top soil and storage layer; (b) profile of root density with data collected from four soil pits; (c) hydraulic conductivity versus volumetric water content; (d) temporal relationship of leaf-area index as represented in *WinUNSAT-H*; K_s = saturated hydraulic conductivity; K_θ = unsaturated hydraulic conductivity; R_d = root length density; z = depth (m); a , b , and c = empirical shape parameters.

Table 2. Compilation of Meteorological Data Resources, Accessibility, and Available Data

Resource	URL	Access ^a	Data type ^b
National solar radiation database	rredc.nrel.gov/solar/old_data/nsrdb/	Free: hourly data ^c	S, P, W, CC, DP, RH, O
NOAA national climate data center	ncdc.noaa.gov	Free: day, month, season, annual data from NCDC archive	T, P, W, CC, DP, RH, O
Weathersource	weathersource.com	Free: monthly and annual summaries; at cost: extended daily and hourly reports	T, P, W, CC, DP, RH, O
WeatherSpark	weatherspark.com	At cost: hourly, daily, monthly weather station data	T, P, W, CC, DP, RH, O
Weather warehouse	weather-warehouse.com	At cost: weather station data	T, P, W, CC, DP, RH, O
Western regional climate center	wrcc.dri.edu	Free: monthly and daily averages; daily measurements	T, P, W, DP, RH, S, O

^aFree access may not apply to general public; free access applicable to universities and other public agencies.

^bT = temperature; P = precipitation; W = wind speed; CC = cloud cover; DP = dew point; S = solar radiation; RH = relative humidity; O = other data also available.

^cSolar radiation measured at select stations; otherwise modeled.

Boundary and Initial Conditions

An atmospheric flux boundary condition corresponding to infiltration rate or evaporation rate was applied at the surface (Fig. 1) as described in Fayer (2000). Runoff at the surface was defined as the difference between precipitation and infiltration, which is commonly referred to as the “infiltration capacity method” (Khire et al. 1999). Percolation was defined as the flux from the base of the cover. The boundary condition at the base of the cover was set as a unit gradient (Fig. 1), which results in slight overpredictions of percolation (Khire et al. 1999).

An initialization simulation was conducted using data from 2004 run 5-year sequentially (i.e., the same data set each year) to obtain a realistic initial distribution of volumetric water content and matric potential throughout the cover profile to use as the initial condition, as recommended in Albright et al. (2010). Average annual precipitation for Missoula, Montana was 337 mm from 1949 to 2010. The annual precipitation in 2004 was 355 mm. Actual daily T_{\max} and T_{\min} for 2004 were similar, on average, compared to average daily temperatures during 1971–2000. Thus, data from 2004 were used to represent a typical year within the 20-year period and also favor a wetter initial soil profile such that percolation would not be underestimated. The profile of matric potential from the end of this initialization simulation period was used as the initial condition in Year 1 for all 20-year water balance model simulations in the study. For each year subsequent to Year 1 (i.e., Year 2, 3, 4, etc.), the soil moisture potential profile at the end of a given year was used as the initial conditions for the subsequent year (e.g., end-of-year soil potential for Year 1 = initial conditions for Year 2).

Spatial and Temporal Discretization

The nodal spacing was set at 1 mm at the boundaries and expanded to as much as 40 mm using a maximum expansion factor of 1.5. The nodal spacing was selected to minimize mass balance errors while maintaining reasonable CPU times. The mass balance criterion was selected so that error in water content at any node did not exceed 10^{-4} . This mass balance criterion resulted in mass balance errors less than 0.1%. A maximum time step of 0.25 h and a minimum time step of 10^{-4} h were used for the simulations.

Simulation Strategy

An initial set of hydrologic predictions was obtained using the complete 20-year daily MET data set as input to *WinUNSAT-H*. This data set is referred to as the actual data herein and is used as

a baseline for comparison with all other model simulations. Subsequent simulations were conducted by replacing the actual data for certain variables in the 20-year data record with surrogate data, as is done in practice when the input data record contains missing data. Predictions made using MET data records incorporating surrogate data were compared to the predictions made with actual data to assess how replacing missing data with surrogates affects water balance quantities.

The simulations that incorporated surrogate MET data were conducted in two phases. In the first phase, the MET data variables T_{dew} , R_s , wind speed, and cloud cover were replaced with daily averages for the 20-year modeling period to simulate a strategy where long-term averages are used to replace missing data. This first phase of the study included simulations where a single MET variable was substituted with averages to assess the effect of individual MET variables on hydrologic predictions as well as a multiple-variable substitution to assess the combined effect of replacing all MET variables (i.e., T_{dew} , R_s , wind speed, and cloud cover) with long-term averages. In the second phase, the MET data variables T_{dew} , R_s , wind speed, and cloud cover were replaced with estimates from empirical models or historical data compilations. The objective of the second phase was to assess the impact of surrogate data on water balance predictions in the event that data are not available for T_{dew} , R_s , wind speed, and cloud cover.

Impact of Using Long-Term Averages for Missing Meteorological Data

A summary of average water balance quantities predicted using the actual data set is in Table 3. Average water balance quantities for the MET data sets with 20-year daily averages used to replace one or more of the MET variables are also in Table 3.

Temporal trends of annual ET, average soil water storage (SWS), and annual percolation for simulations conducted with actual data, all single-variable substitutions, and the multiple-variable substitution are shown in Fig. 3. Annual precipitation is shown along with annual ET in Fig. 3(a). Soil-water storage was obtained by spatially integrating the distribution of water content in the cover profile. The average SWS in Fig. 3 is the arithmetic average of all daily SWS computed during a given calendar year.

There is a general correspondence between annual precipitation and annual ET during the 20-year model simulation period [Fig. 3(a)], which is expected given the predominance of ET in the water balance of water balance covers in semiarid climates (Apiwantragoon et al. 2014). During the first four years of analysis,

Table 3. Summary of Model Sets Conducted Using Averaged Meteorological (MET) Data as Surrogate Input and Corresponding Average Water Balance Characteristic for the 20-Year Analysis

Model set description	Averaged MET data used in model	Water balance characteristics from 20-year analysis						Two-tailed p -statistic for percolation	
		Annual runoff (mm)	Annual ET (mm)	Annual percolation (mm)	Average SWS (mm)	Peak SWS (mm)	Percent precipitation as runoff (%)	Two-sample t -test ^a	Rank-sum test
Actual data	—	0.21	328.6	2.36	151.1	199.4	0.06	—	—
Replace one variable	Solar radiation	0.13	329.3	1.95	146.9	194.6	0.04	0.54	0.47
with average data	Dew point temperature	0.03	329.9	1.71	146.4	190.5	0.01	0.30	0.22
	Wind speed	0.25	327.6	3.25	154.7	206.2	0.08	0.42	0.52
	Cloud cover	0.22	328.6	2.37	151.2	199.5	0.06	0.99	0.94
Replace all variables	Solar, dew point, wind, and cloud	0.01	330.5	1.78	143.9	189.4	0.00	0.42	0.14

Note: ET = evapotranspiration; MET = meteorological; SWS = soil water storage.

^aTwo-sample t -test assuming unequal variances to assess similarity in annual percolation between actual data and simulations with average MET as surrogates.

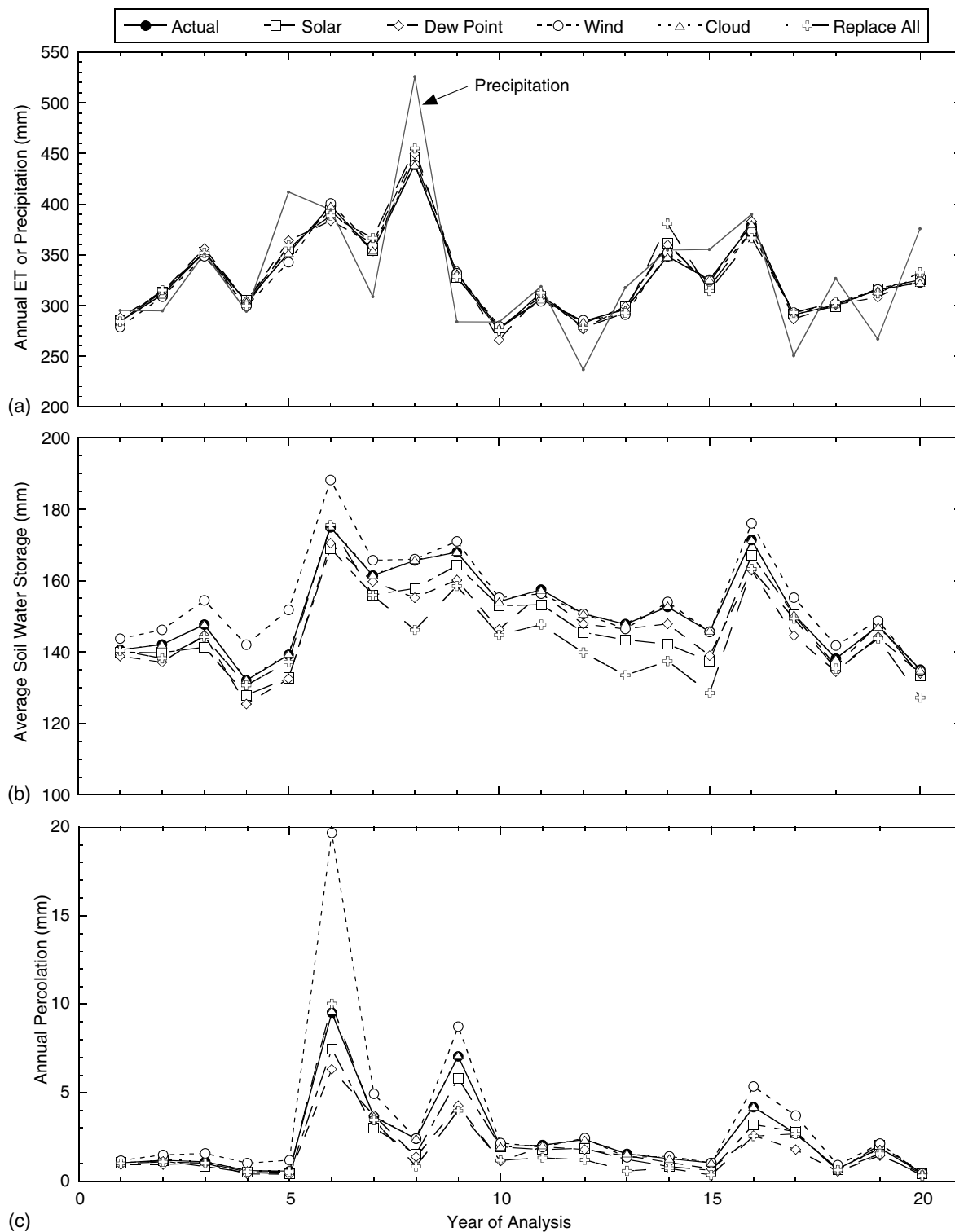


Fig. 3. Temporal relationships of (a) annual evapotranspiration (ET) and precipitation; (b) average soil-water storage; (c) annual percolation for single-variable substitution model simulations as well as the multiple-variable substitution model (replace all)

precipitation and ET are comparable [Fig. 3(a)], SWS remains relatively constant [Fig. 3(b)], and annual percolation is low [≈ 1 mm/year, Fig. 3(c)]. Limited percolation was also predicted in Year 5; however, precipitation in Year 5 was greater than ET and SWS increased modestly relative to Year 4. Average SWS increased substantially in Year 6, causing an increase in percolation for all simulations. Percolation remained higher until Year 15, when SWS returned to the initial level. The trends of increased

percolation during periods of elevated SWS are similar between the actual data simulation and all MET-variable substitutions (Fig. 3).

Annual percolation predicted for each year for the simulations with single-variable and multiple-variable substitutions are normalized with respect to percolation predicted using actual data in Fig. 4. Each bin in Fig. 4 contains 20 points corresponding to annual percolation predicted for each year in the 20-year record. Dashed horizontal lines in Fig. 4 represent the average normalized percolation

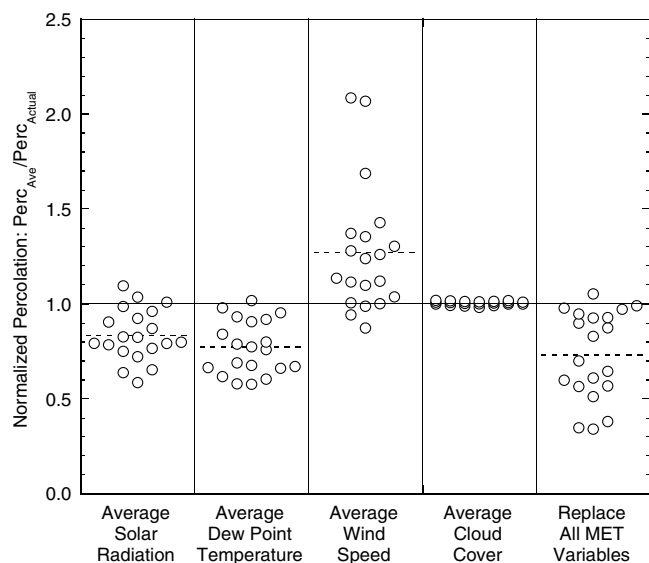


Fig. 4. Dot plot of normalized percolation, whereby normalizations were computed between percolations predicted with averaged meteorological data used as surrogate in single-variable substitutions or the multiple-variable substitution (PercAve) and percolation predicted with actual data (PercActual) for each year of the 20-year analysis

rate over the 20-year record in each bin. The most comparable predictions of percolation for a single MET variable were obtained when cloud cover was replaced with average data, which is evident by the cluster of data points near the 1.0-normalization line in Fig. 4.

Two-sample t -tests were conducted at the 5% significance level to compare annual percolation predicted using the actual data and annual percolation predicted with each single-variable and multiple-variable substitution model (Table 3). T -tests assume normality in a population distribution, which was approximately valid for all percolation rate compilations with modest skew in the distributions towards high percolation rates [e.g., Years 6 and 9 of the simulations, Fig. 3(c)]. Rank-sum tests also were conducted on annual percolation rates similar to the t -tests, and were used as a complimentary statistical assessment that can be more effective when outliers are present [e.g., high percolation rates in Years 6 and 9, Fig. 3(c)]. The t -tests were conducted under the null hypothesis that there is no difference in mean annual percolation; rank-sum tests were conducted under the null hypothesis that percolation rates from actual data and MET substitution models constituted identical population distributions (i.e., there was no effect of surrogate MET data on the magnitude of percolation).

Overall, all single-variable substitutions using average MET data as surrogate data as well as the multiple-variable substitution yielded predictions of annual percolation that were statistically similar to percolations predicted using actual data (i.e., two-tailed p -statistics $\gg 0.05$ for all scenarios, Table 3). That is, using surrogate input did not significantly impact predictions of percolation rate. The two-tailed p -statistics for cloud cover are the largest of the simulations that were conducted (Table 3), and indicates a higher degree of similarity compared to predictions obtained from the single-variable substitutions using average R_s , T_{dew} , or wind speed.

Changes in annual percolation (Fig. 3) for the single-variable and multiple-variable substitutions are driven by changes in predicted ET and corresponding changes in SWS. Normalized percolation versus normalized ET and normalized percolation versus normalized SWS for all MET-variable substitutions are shown in Figs. 5(a and b). Similar to Fig. 4, the normalizations

for percolation, ET, and SWS were computed as the quotient of the quantity predicted with average data used as a surrogate relative to the quantity predicted with the actual data. Normalized percolation and normalized ET for the average cloud-cover simulation all cluster around the 1.0:1.0 origin point in Fig. 5(a), indicating that replacing the cloud-cover data had negligible impact on the ET predictions. Correspondingly, there was negligible change in predicted SWS or predicted percolation when using average cloud-cover data in lieu of actual data [Fig. 5(b)].

Systematic changes were observed between percolation, ET, and SWS for the simulations with single-variable substitutions of average R_s , T_{dew} , and wind speed. Simulations with single-variable substitution using average wind or average T_{dew} yielded predicted annual percolation rates that differ the most from predictions obtained with actual data, as indicated by the lower p -statistics (Table 3). Using average T_{dew} led to 27% lower predicted percolation, on average, compared to percolation predicted with actual data. Lower percolation was predicted using average T_{dew} because greater ET was predicted that led to lower SWS (Fig. 3). In contrast, percolation predicted using average wind speed was 38% higher, on average, than percolation predicted using actual data (Table 3) because lower ET was predicted, which led to higher SWS. Although normalized ET for the average R_s simulation cluster around 1.0 [Fig. 5(a)], the lower SWS predicted using averaged R_s was attributed to the higher ET that lowered predicted percolation [Fig. 5(b)].

The positive trend between normalized percolation and normalized SWS in Fig. 5(b) indicates that higher percolation events are concurrent with higher SWS (i.e., wetter soil) and are independent of the substituted MET data. Soil water storage increases when precipitation exceeds ET in a given year, and in particular, when subsequent years align with higher precipitation relative to ET (e.g., Years 5 and 6 and Years 15 and 16 as shown in Fig. 3). Normalized percolation and normalized SWS are plotted with respect to normalized ET of the previous year in Figs. 5(c and d). Although scatter still exists in Figs. 5(c and d), a general negative correspondence can be observed, which indicates that higher SWS and higher percolation are more likely to occur when ET predicted in the previous year is lower relative to ET predicted with actual data. Thus, the prior year ET appears to have a more dominant impact on percolation and SWS in a given year, which helps to explain the absence of a trend between normalized percolation and normalized ET in Fig. 5(a).

Relationships between annual percolation and average SWS, the ratio of precipitation to ET_p , and ratio of prior year precipitation to ET_p are shown in Fig. 6. A positive, exponential trend of annual percolation versus average SWS is evident in Fig. 6(a) regardless of the substituted MET data used in a given simulation. This behavior is attributed to a reduction in available storage capacity as SWS increases, whereby precipitation events concurrent with elevated SWS lead to higher percolation. Trends between percolation and SWS in Fig. 6(a) are unique for the soil cover considered in this modeling exercise, and predicting percolation based on SWS estimates should account for site-specific conditions. The uniqueness of the single trendline in Fig. 6(a) for all model simulations suggests that the relationship between annual percolation and average SWS can be used as a check on percolation predicted using surrogate data for a given site.

There was no statistically significant trend in the relationship of annual percolation versus ratio of precipitation to ET_p [Fig. 6(b)]; however, a positive and statistically significant trend was determined for the relationship between annual percolation versus the ratio of prior year precipitation to ET_p [Fig. 6(c)]. A higher precipitation to ET_p ratio indicates a greater amount of water present as compared to energy available to remove water from the cover

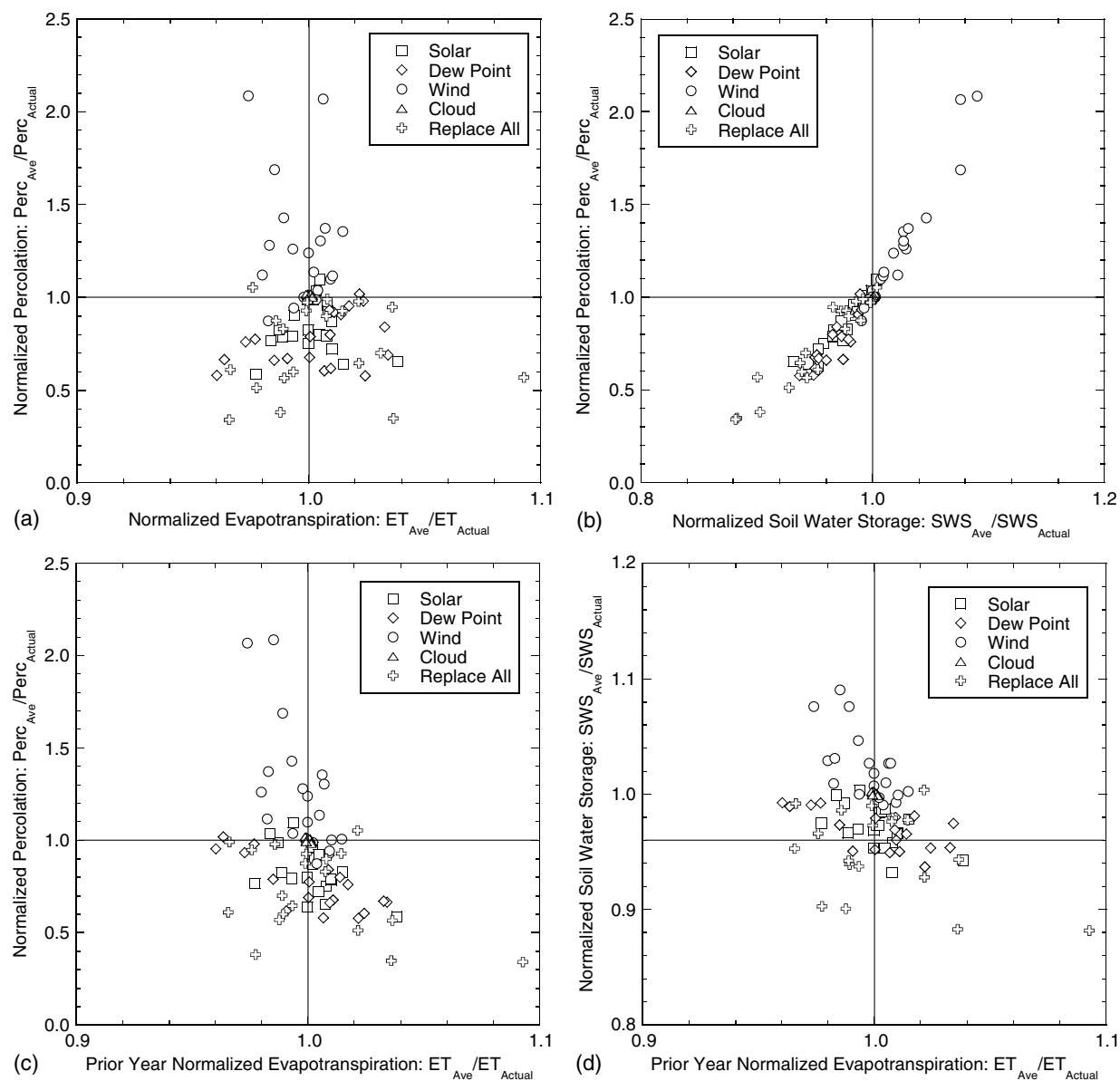


Fig. 5. Comparisons of (a) normalized percolation (Perc) to normalized evapotranspiration (ET); (b) normalized Perc to normalized soil water storage (SWS); (c) normalized Perc to normalized ET of the prior year; (d) normalized SWS to normalized ET of the prior year for single-variable and multiple-variable substitutions; all normalizations are between predictions made with given set of averaged meteorological data used as surrogate input ("Ave" subscript) and predictions made with the actual data (*actual* subscript)

system. Higher precipitation to ET_p ratios do not necessarily indicate a propensity for increased percolation [Fig. 6(b)], since SWS initially may be low during years of high precipitation. An increase in precipitation is required to increase SWS and subsequently lead to elevated percolation when precipitation is concurrent with high SWS. This phenomenon is apparent in the positive trend between percolation and the ratio of prior year precipitation to ET_p [Fig. 6(c)]. Elevated precipitation in the prior year results in elevated SWS at the end of the prior year, lower storage capacity in the following year, and greater potential to exceed the SWS in the following year if the precipitation is elevated.

The simulation with multiple-variable substitutions (i.e., Replace All in Figs. 4–6) underpredicted percolation by 25% (0.25 mm/year), on average, relative to percolation predicted with actual data (Table 3). This was largely due to the effect of average R_s and average T_{dew} (Table 3) resulting in higher ET and therefore lower SWS and lower percolation [Figs. 4, 5(b), and 6(a)]. The

overprediction of percolation using average wind speed and cloud cover mitigates some of the underprediction caused by average T_{dew} in the multiple-variable substitution prediction (Table 3). However, the underpredicted percolation using all averaged MET data as surrogates is not ideal from a perspective of predicting percolation that is representative of actual data. More-accurate estimates of daily R_s and T_{dew} that reflect daily climatic conditions will result in predictions of percolation that are closer to those obtained with actual data.

Impact of Using Estimates for Missing Meteorological Data

Estimation Techniques

Techniques to estimate T_{dew} , R_s , wind speed, and cloud cover were identified that did not require additional MET data relative to the

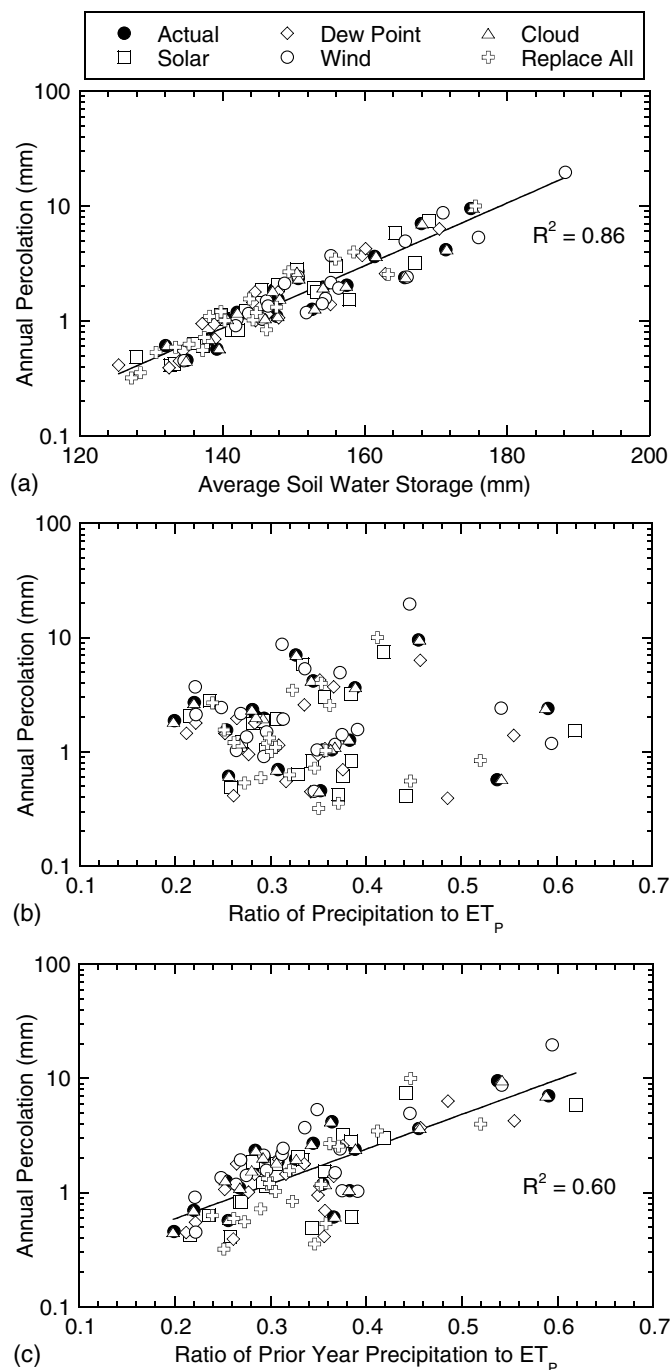


Fig. 6. Relationships of annual percolation versus: (a) average soil water storage; (b) ratio of precipitation to potential evapotranspiration (ETP); (c) ratio of prior year precipitation to ETP for actual data and all single-variable and multiple-variable substitutions; regression lines are included for statistically significant trends and are regressed through all data points

MET data required in *WinUNSAT-H*. Estimated MET data were compared with actual MET data to assess the accuracy of estimation techniques and anticipated effects on hydrology predictions from water balance models. These comparisons were used to identify appropriate estimation techniques for surrogate MET data that were then incorporated into water balance modeling. Complete 20-year model simulations were completed with appropriate MET data estimation strategies to assess the viability of using estimated

MET data to generate representative hydrologic predictions for the water balance cover evaluated in this study.

Dew Point Temperature Estimation

Dew point temperature was estimated based on (1) the assumption that $T_{\text{dew}} = T_{\text{min}}$, (2) the assumption that $T_{\text{dew}} = T_{\text{min}} - 2^{\circ}\text{C}$, and (3) a model described in Hubbard et al. (2003). Although T_{min} can be a reasonable estimate of T_{dew} (Allen et al. 1998), T_{min} is often higher than T_{dew} in arid and semiarid climates (Kimball et al. 1997). Thus, ET_p may be underestimated when computed using the assumption that $T_{\text{dew}} = T_{\text{min}}$. Allen et al. (1998) recommend that T_{dew} can be more accurately estimated as $T_{\text{min}} - 2$ to 3°C . For this study, simulations were conducted with $T_{\text{dew}} = T_{\text{min}}$ and $T_{\text{dew}} = T_{\text{min}} - 2^{\circ}\text{C}$.

Hubbard et al. (2003) recommend computing T_{dew} as

$$T_{\text{dew}} = -0.0360(T_{\text{avg}}) + 0.9679(T_{\text{min}}) + 0.0072(T_{\text{max}} - T_{\text{min}}) + 1.0119 \quad (6)$$

where T_{avg} = average of T_{max} and T_{min} . This empirical model was developed using six climate stations in the Northern Great Plains of the United States, with climates ranging from subhumid to semi-arid. Hubbard et al. (2003) report that their model [Eq. (6)] yielded $R^2 \geq 0.90$ for predictions of T_{dew} at five additional sites and is applicable to a broad range of climatic conditions.

Solar Radiation Estimation

A detailed review of available empirical models to estimate R_s is presented in Besharat et al. (2013). They report that a model developed by Hargreaves and Samani (1982) yielded the most accurate R_s estimates among the temperature-based R_s modeling techniques evaluated. A temperature-based model presented in Annandale et al. (2002) builds off the Hargreaves and Samani (1982) model to incorporate site elevation and account for potential effects of varying atmospheric thickness. Almorox (2011) evaluated the Hargreaves and Samani (1982) and Annandale et al. (2002) models for estimating R_s at a site south of Madrid, Spain and reported that both models yielded comparable and accurate estimates of R_s for situations when only temperature data were available. Thus, the empirical R_s models in Hargreaves and Samani (1982) and Annandale et al. (2002) were considered in this study.

Solar radiation in the Hargreaves and Samani (1982) model is calculated as

$$R_s = R_a[k_{rs}(T_{\text{max}} - T_{\text{min}})^{1/2}] \quad (7)$$

where R_a = extraterrestrial radiation; and k_{rs} = empirical constant that is equal to 0.16 for interior regions and 0.19 for coastal regions (Hargreaves 1984; Besharat et al. 2013). Solar radiation estimates for this study were initiated with $k_{rs} = 0.16$ since Missoula, Montana can be considered an interior region. An optimization of k_{rs} also was conducted based on a least-squares analysis via comparison between actual daily R_s for the 20-year MET data period and R_s computed with Eq. (7). This optimization yielded $k_{rs} = 0.143$.

Solar radiation in the Annandale et al. (2002) model is calculated as

$$R_s = R_a[k_{rs}(1 + z \cdot 2.7 \times 10^{-5})(T_{\text{max}} - T_{\text{min}})^{1/2}] \quad (8)$$

where z = site elevation in meters; and $k_{rs} = 0.16$. Elevation of the site was set equal to 978.0 m, which is an average elevation for the surrounding site area. Factoring in this site elevation yields a multiplicative constant of 0.164, which is analogous to the single k_{rs} in Eq. (7).

Extraterrestrial radiation (R_a), required in Eqs. (7) and (8), is defined as solar radiation received on a horizontal surface outside

of Earth's atmosphere (Allen et al. 1998). Extraterrestrial radiation can be calculated as

$$R_a = \left(\frac{1}{\pi}\right) G_{sc} \cdot d_r [\omega_s \cdot \sin(\lambda) \sin(\delta) + \cos(\lambda) \cos(\delta) \sin(\omega_s)] \quad (9)$$

where

$$d_r = 1 + 0.033 \cdot \cos\left(\frac{2 \cdot \pi}{365} J\right) \quad (10)$$

$$\delta = 0.409 \cdot \sin\left(\frac{2 \cdot \pi}{365} J - 1.39\right) \quad (11)$$

$$\omega_s = \cos^{-1}[-\tan(\lambda) \tan(\delta)] \quad (12)$$

and where G_{sc} = solar constant ($118.11 \text{ MJ/m}^2 \cdot \text{d}$); d_r = inverse relative distance between the Earth and Sun; δ = solar declination (degrees); λ = latitude of the site (degrees); ω_s = hour angle of the Sun (degrees); and J = Julian day.

Cloud Cover Estimation

Campbell (1985) recommended that cloud cover (c) can be estimated as

$$c = 2.33 - 3.33T_t \quad (13)$$

where c = cloud cover; and T_t = transmission coefficient, which is taken as the ratio of measured solar radiation to potential solar radiation (i.e., R_s/R_a). Cloud cover computed with Eq. (13) must be constrained to range between 0.0 and 1.0. No other means for estimating cloud cover were identified and no compilations of historic cloud-cover data were found for the site considered in this study.

Wind Speed Estimation

Wind speed was estimated using two historical data trends: (1) monthly local average and (2) annual global average. For the monthly local average method, all daily data within a given month were replaced with a single monthly average wind speed (e.g., wind speed = 2.3 m/s for every day in January). Monthly average wind speeds for Missoula, Montana were obtained from the Western Regional Climate Center (Reno, Nevada) and were based on measurements made during 1996 to 2006. For the annual average method, all daily wind speeds were assumed equal to 2 m/s,

which is the global average wind speed reported in Allen et al. (1998) based on data collected from over 2000 weather stations. No empirical estimation technique was found for wind speed that was applicable to the site and modeling scenario evaluated in this study.

Comparison of Actual versus Estimated Meteorological Data

A comparative assessment between the different MET data estimation techniques was conducted to identify appropriate techniques for generating surrogate MET data for use in water balance modeling. A statistical summary of residuals, computed as the difference between estimated and actual MET data, is included in Table 4. Meteorological parameter estimation techniques that yield estimates with an average residual closer to zero and lower standard deviation are more representative of actual data. Additionally, an estimate of a given MET parameter should tend towards predicting water balance quantities closer to reality, and that the prediction of percolation should be greater than or equal to percolation predicted using actual data.

Comparison plots of estimated versus actual MET data for the selected MET parameter estimation techniques for T_{dew} , R_s , and wind speed are in Fig. 7. Assuming $T_{\text{dew}} = T_{\text{min}}$ yielded the closest estimate to actual T_{dew} compared with the other two techniques (Table 4). The average residual is 0.85 when $T_{\text{dew}} = T_{\text{min}}$, indicating that T_{dew} is overestimated when assumed equal to T_{min} . This overestimate is shown graphically in Fig. 7(a) based on the majority of data plotting above the 1:1 line. An overestimate of T_{dew} decreases ET_p [Eq. (2)] based on a smaller difference between saturated and actual vapor pressure (i.e., $e_a - e_d$ in Eq. (2)). When ET_p is lower, actual ET is lower, which leads to greater SWS and predicted percolation exceeding the percolation predicted using actual data.

The two estimation methods for wind speed both yielded a negative average residual (Table 4), indicating that both methods underestimate wind speed relative to actual data. Underestimating wind speed in Eq. (2) leads to an underprediction of ET_p , which will result in an overprediction of percolation. Thus, from a perspective of overpredicting percolation, estimating wind speed based on local monthly averages or the global average would be appropriate, at least for the site evaluated in this study. Local monthly average wind speeds were selected as the surrogate data-estimation technique for this study based on an average bias and

Table 4. Statistical Summary of Residuals between Estimated Meteorological (MET) Parameters and Actual MET Parameters

MET parameter	Estimation technique	Statistical metrics				
		Average	Median	Maximum	Minimum	Standard deviation
Dew point temperature (K)	$T_{\text{dew}} = T_{\text{min}}$	0.85	0.39	15.00	-7.61	2.93
	$T_{\text{dew}} = T_{\text{min}} - 2^\circ\text{C}$	-1.15	-1.61	13.00	-9.61	2.93
	Hubbard et al. (2003)	1.66	1.26	14.76	-5.65	2.67
Solar radiation (langleys)	H&S, $k_{rs} = 0.16$	44.6	35.7	397.9	-220.6	73.3
	H&S, $k_{rs} = 0.143$	4.5	2.3	323.6	-276.3	72.0
	Annandale et al. (2002)	54.3	43.7	415.9	-207.1	74.7
Wind speed (m/s)	Local monthly average	-0.22	0.03	2.53	-8.29	1.35
	Global average	-0.33	-0.15	2.00	-8.06	1.42
Cloud cover (tenths) ^a	Actual data	-0.01	0.00	0.68	-1.00	0.19
	H&S, $k_{rs} = 0.16$	-0.12	-0.08	0.98	-1.00	0.24
	H&S, $k_{rs} = 0.143$	0.03	0.02	1.00	-1.00	0.23

Note: H&S = Hargreaves and Samani (1982) model; k_{rs} = empirical constant in H&S model; T_{dew} = dew point temperature; T_{min} = minimum air temperature; residuals were computed as the difference between estimated MET parameter and actual MET parameter; Kelvin was used to compute residuals to avoid issues with negative and positive degrees Celsius; statistics are based on comparison of 7,305 daily MET data comparisons.

^aCloud cover estimated based on Eq. (12), which is embedded in *WinUNSAT-H*; estimation techniques refer to the method of estimating R_s , which is used in the cloud cover calculation; actual R_s (i.e., actual data) is included for comparison.

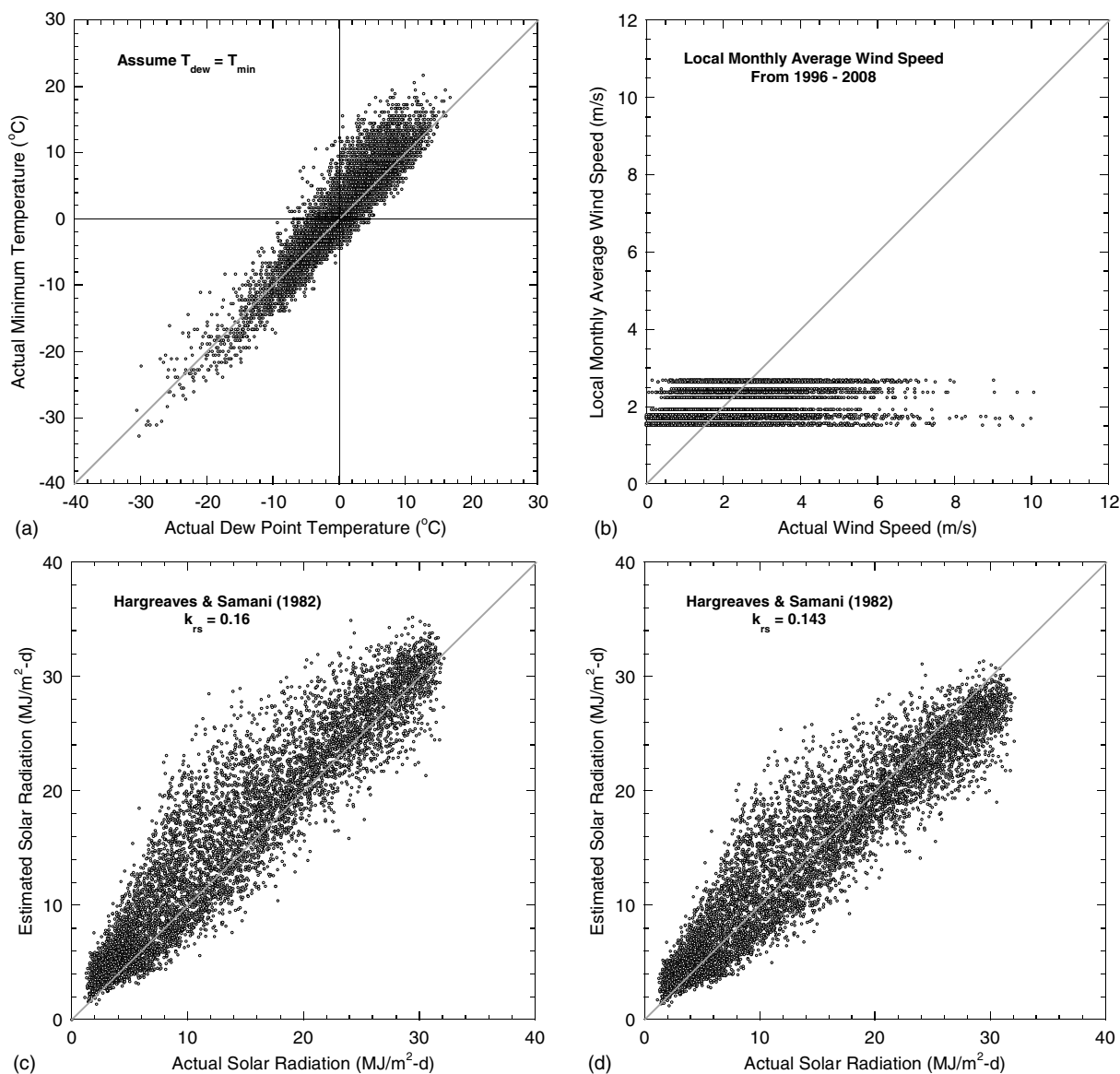


Fig. 7. Relationships between estimated meteorological data and actual meteorological data for (a) dew point temperature assumed equal to minimum temperature; (b) wind speed estimated as local average monthly wind speed; (c) solar radiation estimated with $k_{rs} = 0.16$ in the Hargreaves and Samani (1982) model; (d) solar radiation estimated with $k_{rs} = 0.143$ in the Hargreaves and Samani (1982) model

Table 5. Summary of Model Sets Conducted with Estimated Meteorological Data Used as Surrogate Input and Corresponding Average Water Balance Characteristics for the 20-Year Analysis

Model set description	Averaged MET data used in model	Water balance characteristics from 20-year analysis						Two-tailed p-statistic for percolation	
		Annual runoff (mm)	Annual ET (mm)	Annual percolation (mm)	Average SWS (mm)	Peak SWS (mm)	Percent precipitation as runoff (%)	Two-sample t -test ^a	Rank-sum test
Actual data	—	0.21	328.6	2.36	151.1	199.4	0.06	—	—
Simulation 1 (S1)	$T_{dew} = T_{min}$, R_s via H&S model, local wind,	0.07	328.9	2.43	148.8	198.4	0.02	0.94	0.52
Simulation 2 (S2)	and cloud cover via Eq. (13); S1, $k_{rs} = 0.16$; S2, $k_{rs} = 0.143$	0.12	327.4	3.44	155.6	207.6	0.04	0.32	0.44

Note: ET = evapotranspiration; MET = meteorological; SWS = soil water storage. T_{min} = minimum air temperature; T_{dew} = dew point temperature; R_s = solar radiation; H&S = Hargreaves and Samani (1982) solar radiation model; Local wind = monthly average wind speed for Missoula, Montana from 1996 to 2006; k_{rs} = empirical constant in H&S model.

^aTwo-sample t -test assuming unequal variances to assess similarity in annual percolation between actual data and simulations with surrogate data.

standard deviation closer to zero relative to global average wind speeds (Table 4).

Estimating R_s with the models outlined in Eqs. (7) and (8) both lead to overestimates of R_s , as shown by the positive average residuals in Table 4. An overestimate of R_s will result in an overprediction of ET_P [Eq. (2)], underprediction of SWS, and

an underprediction of percolation. The Annandale et al. (2002) approach yielded the largest positive residual and largest standard deviation, and thus, was not considered an appropriate R_s estimation technique for this study. Optimizing k_{rs} in the Hargreaves and Samani model [Eq. (7)] via least squares analysis reduced the average residual relative to using $k_{rs} = 0.16$ (Table 4). This shift in

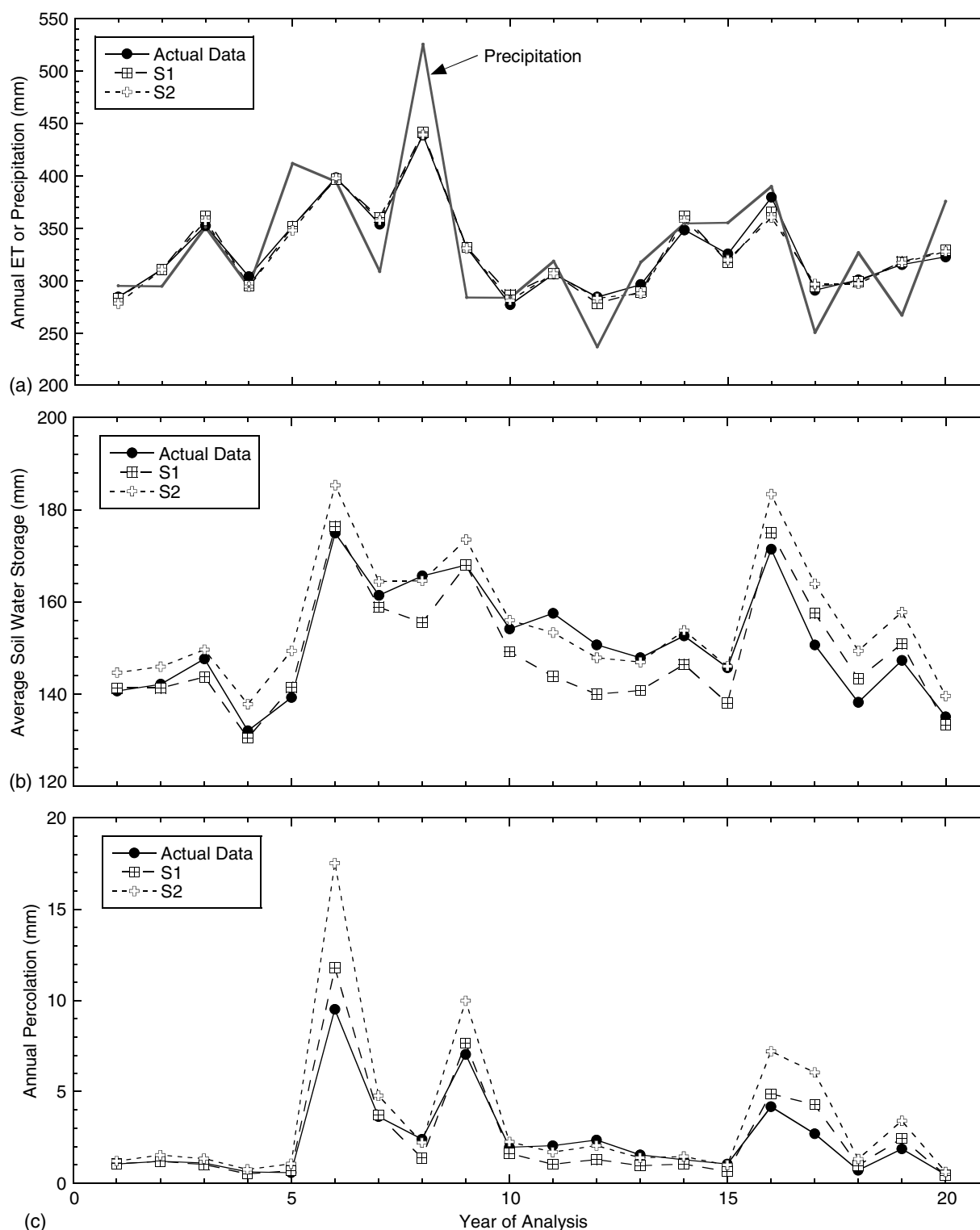


Fig. 8. Temporal relationships of (a) annual evapotranspiration (ET) and precipitation; (b) average soil water storage; (c) annual percolation for the actual data simulation and simulations using empirical estimates of meteorological data as surrogate input (S1 = Simulation 1 and S2 = Simulation 2; techniques outlined in Table 5)

residuals closer to zero is shown graphically in Figs. 7(c and d). Using $k_{rs} = 0.143$ shifts the estimated R_s data closer to the 1:1 line, which will yield more-accurate predictions of ET_p [Eq. (2)] relative to using $k_{rs} = 0.16$.

Estimating cloud cover with Eq. (13) depends on the R_s data used as input. Residuals of cloud-cover estimates based on actual R_s as well as R_s predicted with the Hargreaves and Samani (1982) model for both k_{rs} are included in Table 4. An average and median residual near zero were computed for cloud cover estimated with Eq. (13) and actual R_s data, which was anticipated considering R_s and cloud cover are related. The Hargreaves and Samani (1982) model with $k_{rs} = 0.16$ overestimated R_s and led to an

underestimate of cloud cover (Table 4). Decreasing the estimated R_s using the optimized $k_{rs} = 0.143$ led to closer agreement between estimated and actual cloud cover.

Water balance modeling in the event T_{dew} , R_s , wind-speed, and cloud-cover data are not available was completed with the following considerations: (1) $T_{dew} = T_{min}$; (2) R_s estimated with the Hargreaves and Samani (1982) model; (3) daily wind speed set equal to monthly averages; and (4) cloud cover estimated with Eq. (13). Two model simulations were completed with these considerations: Simulation 1 (S1), which included R_s estimated with $k_{rs} = 0.16$, and Simulation 2 (S2), which included R_s estimated with $k_{rs} = 0.143$. Aside from the k_{rs} used to compute R_s in the

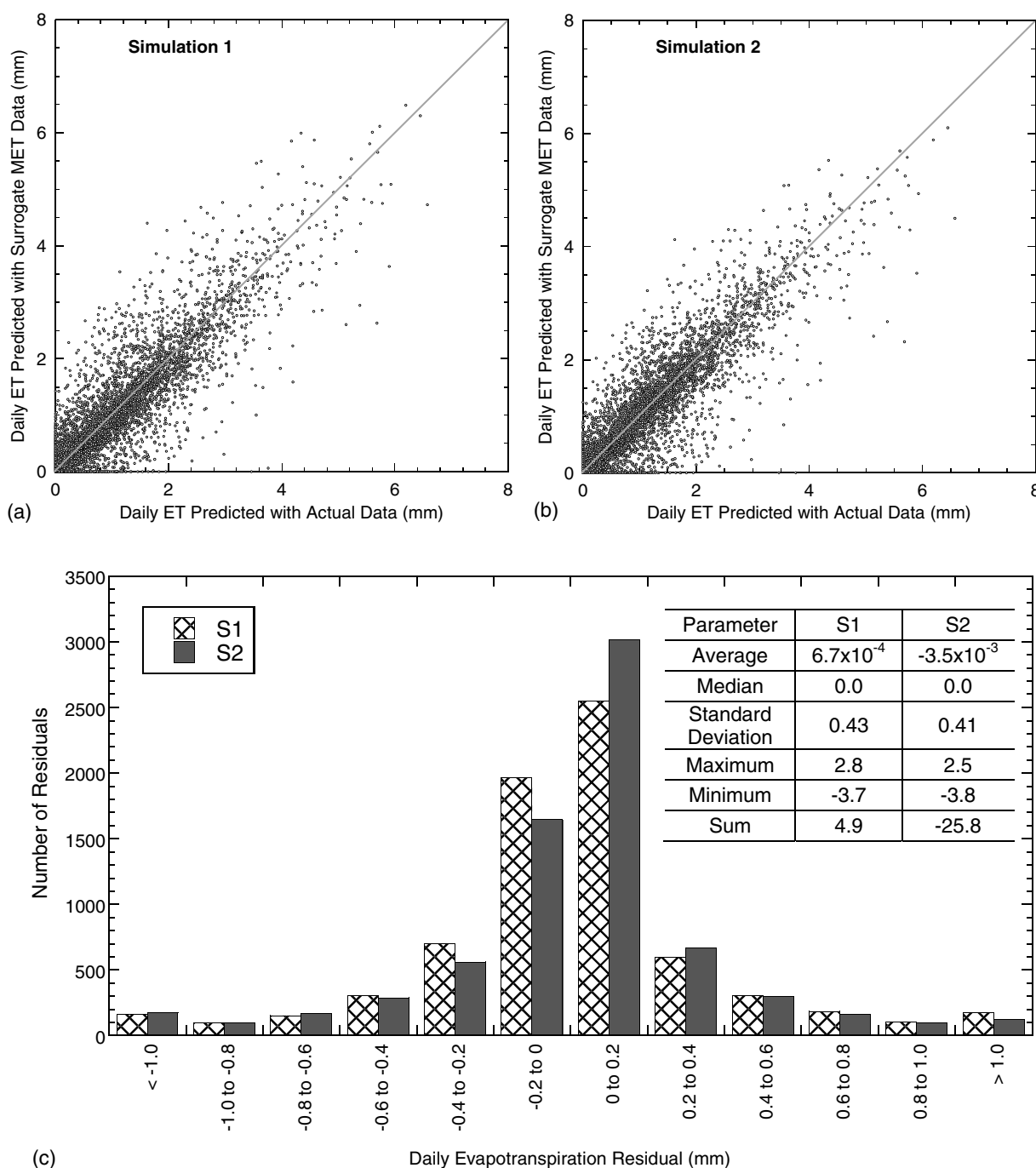


Fig. 9. One-to-one plots of daily evapotranspiration (ET) predicted with: (a) simulation 1 (S1); (b) simulation 2 (S2) versus daily ET predicted with actual data for the 20-year simulation period as well as; (c) the distribution of ET residuals for S1 and S2; residuals were computed as the difference between ET predicted for S1 or S2 and ET predicted with actual data

Hargreaves and Samani (1982) model, all other MET data considerations were the same in S1 and S2. This proposed surrogate MET data estimation technique was intended to yield conservative predictions; that is, lower ET, higher SWS, and higher percolation relative to predictions that would be made using actual data.

Water Balance Predictions Using Estimated Meteorological Data

A summary of the average 20-year water balance characteristics for model simulations S1 and S2 is in Table 5. Temporal trends of annual ET, average SWS, and annual percolation for the actual data simulation and S1 and S2 are in Fig. 8. There is close agreement

between ET predicted for the actual data and for both simulations with estimated MET data used as surrogates [Table 5 and Fig. 8(a)]. The average annual ET for the 20-year period for S2 was 1.5 mm less than in S1, which is attributed to the lower k_{rs} (0.143 versus 0.16) used to predict R_s with Eq. (7). This modest decrease in ET for S2 contributed to an increase in average SWS [Table 5 and Fig. 8(b)] and increase in annual percolation [Table 5 and Fig. 6(c)] relative to S1 and the simulation with actual data.

Water balance simulations S1 and S2 both overpredicted annual percolation slightly over the 20-year period compared to the actual data (Table 5). Simulation 2 yielded predictions of annual percolation that were closer to or overpredicted percolation relative to percolation predicted with actual data [Fig. 8(c)]. Thus, the

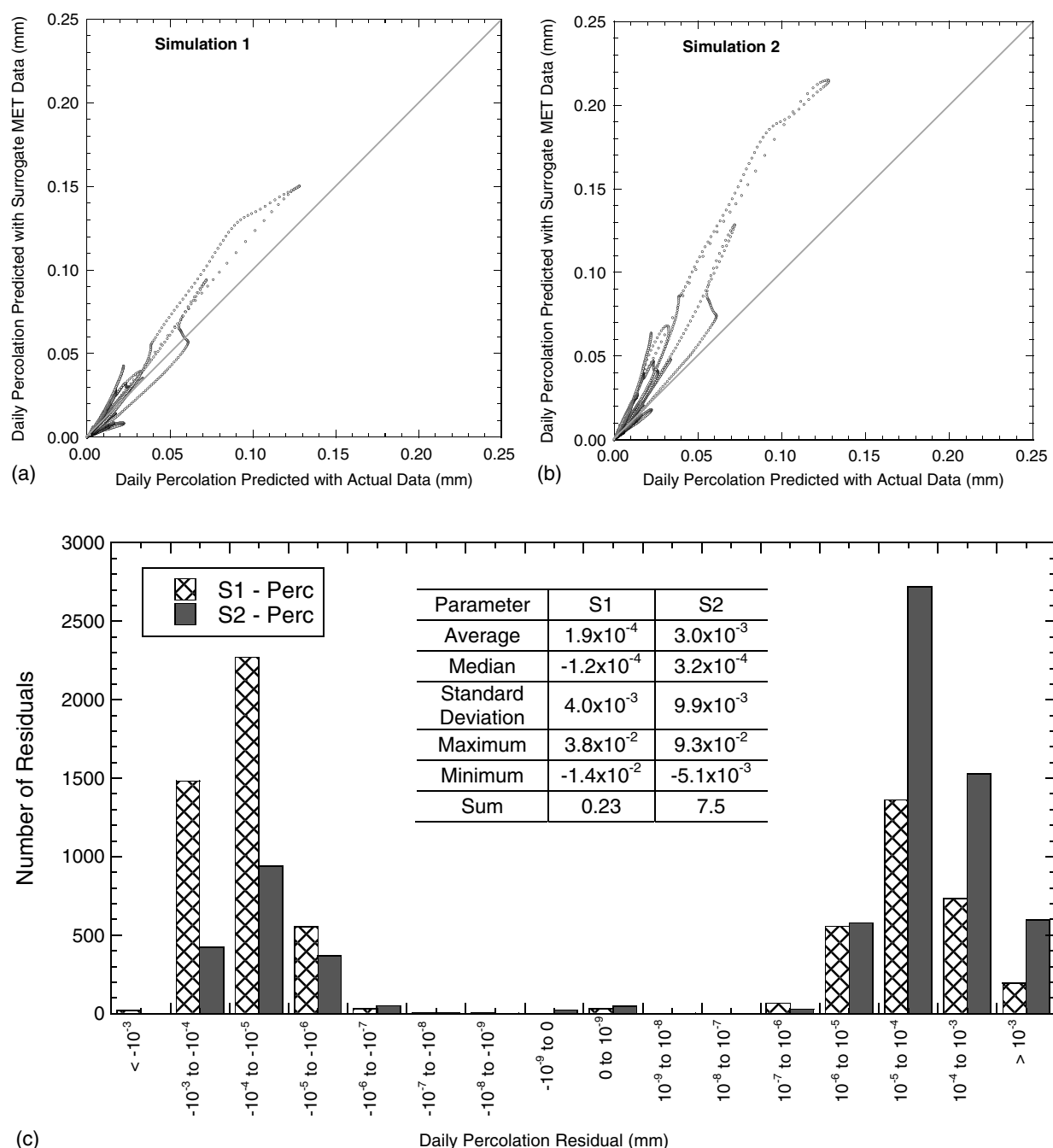


Fig. 10. One-to-one plots of daily percolation predicted with (a) Simulation 1 (S1) (b) Simulation 2 (S2) versus daily percolation predicted with actual data for the 20-year simulation period as well as (c) the distribution of percolation residuals for S1 and S2. Residuals were computed as the difference between percolation predicted for S1 or S2 and percolation predicted with actual data

surrogate MET data estimation technique used in S2, with an optimized $k_{rs} = 0.143$, is more appropriate for generating annual percolation predictions that are less likely to underpredict percolation.

One-to-one plots of daily ET predicted with S1 and S2 versus ET predicted with actual data as well as the distribution of daily ET residuals for S1 and S2 for the 20-year data set are shown in Fig. 9. Both simulations with surrogate MET data yielded comparable predictions of ET relative to actual data, which is shown by the similar distribution of ET points about the 1:1 lines in Figs. 9(a and b). Residuals for ET were computed as the difference between ET predicted for a given simulation with surrogate MET data (S1 or S2) and ET computed based on actual data. Residuals for both S1 and S2 models are approximately normally distributed about zero with average and median residuals near zero (Fig. 9). This distribution and the accompanying statistics indicate that there is negligible bias when predicting ET using an estimated R_s with $k_{rs} = 0.16$ or 0.143 . The sum of all residuals for S2 is negative (-25.8 mm) compared to S1 (4.9 mm), which contributes to the lower average annual ET (Table 5).

One-to-one plots of percolation predicted with S1 and S2 versus percolation predicted with actual data as well as the distribution of daily percolation residuals for S1 and S2 for the 20-year data set are shown in Fig. 10. The 1:1 comparisons depict a bias for larger daily percolation predictions for S2 as opposed to S1, which was expected considering a larger annual average percolation was obtained using the surrogate data estimation technique in S2 (Table 5). Residuals for percolation were computed as the difference between percolation predicted for a given simulation with surrogate MET data (S1 or S2) and percolation computed based on actual data [Fig. 10(c)]. Statistics of the percolation residuals [Fig. 10(c)] are similar between S1 and S2, with the main difference being a bias towards positive residuals for S2. The use of $k_{rs} = 0.143$ in S2 decreased the predicted R_s [Fig. 7(d)], which reduced ET for S2 relative to actual data (Table 5 and Fig. 9) and led to larger daily predictions of percolation.

Overall, the surrogate MET data-estimation technique outlined herein yielded average annual percolation that was larger relative to percolation predicted with actual data over a 20-year period ($+3\%$ or $+0.07$ mm/year for S1, and $+46\%$ or $+1.08$ mm/year for S2, Table 5). This close agreement between average annual percolation predicted with S1 and S2 suggests that the aforementioned method to generate surrogate MET data is appropriate for water balance modeling at the semiarid site evaluated in this study. The recommended surrogate MET data estimation approach incorporates an assumption that $T_{\text{dew}} = T_{\text{min}}$, R_s estimated based on the Hargreaves and Samani (1982) model, daily wind speeds replaced with local monthly average wind speeds, and cloud cover estimated as a function of solar radiation. The recommended empirical constant in the Hargreaves and Samani (1982) model for interior regions ($k_{rs} = 0.16$) is appropriate for predicting R_s in semiarid regions of the western United States. However, k_{rs} in the Hargreaves and Samani (1982) model may be reduced to yield more conservative overestimates of annual percolation. The 20-year data set evaluated in this study yielded an optimal $k_{rs} = 0.143$, which may be used for water balance modeling completed for comparable semiarid, mountainous regions similar to the site evaluated in this study.

Summary and Conclusions

The effect of using surrogate MET data on hydrological predictions was evaluated with the variably saturated flow code *WinUNSAT-H* for a water balance cover at a municipal solid waste landfill in Missoula, Montana. Hydrology predictions were made for a 20-year

period using (1) a complete set of actual MET data, (2) single-variable and multiple-variable substitutions of average daily MET data as surrogates, and (3) empirical estimates of MET data as surrogates. Although findings from this study are specific to the site evaluated, similar findings should be obtained using other common variably saturated flow codes based on similar principles and at other sites in the semiarid western United States. Generalization to more humid sites, however, requires additional study.

The following conclusions were drawn from this study.

- The effect of using averaged MET data on percolation predicted from a water balance model is related to the influence of the substituted MET parameter on evapotranspiration (ET) and soil water storage (SWS). Thus, methods to estimate missing data that result in an overprediction of ET also result in an underprediction of SWS and an underprediction of percolation. The converse is also true.
- Replacing actual MET data with daily averages of T_{dew} and R_s increased ET, decreased SWS, and led to lower predicted annual percolation relative to using a complete set of actual data. In contrast, replacing wind speed or cloud cover with daily averages decreased ET, increased SWS, and led higher predicted percolation relative to using a complete set of actual data. Replacing all MET data variables with daily averages led to underpredictions of annual percolation (25% or 0.58 mm/year on average) relative to using actual data. Thus, using a compilation of averaged MET data as surrogate input for water balance modeling may underestimate predicted percolation.
- Empirical estimates of MET data (T_{dew} , R_s , wind speed, and cloud cover) that are appropriate for use as surrogate input for water balance modeling include the following: (1) $T_{\text{dew}} = T_{\text{min}}$; (2) R_s estimated with the Hargreaves and Samani (1982) model; (3) daily wind speed set equal to monthly averages; and (4) cloud cover estimated as a function of solar radiation [Eq. (13)]. Using these methods to estimate surrogate MET data led to modest overestimates of annual average percolation (3 and 46%, or 0.07 and 1.08 mm/year) when compared to percolation predicted using actual data.
- Estimating R_s based on Hargreaves and Samani (1982) with their recommended empirical constant (k_{rs}) equal to 0.16 yielded annual average percolation (2.43 mm/year) that was comparable to percolation predicted using actual data (2.36 mm/year). However, percolation predicted from simulations using $k_{rs} = 0.16$ to compute R_s occasionally was underpredicted relative to percolation predicted using actual data. A $k_{rs} = 0.143$ was determined via least squares optimization between estimated R_s and actual R_s . This value of k_{rs} reduced predictions of daily ET, increased average SWS, and increased annual percolation (3.44 mm/year) compared to predictions made with actual data. Thus, the empirical MET data-estimation technique used to generate surrogate input outlined in this study, with R_s predicted based on $k_{rs} = 0.143$, is recommended for predicting annual percolation in water balance models for comparable sites in semiarid, mountainous regions similar to the site evaluated in this study.

Acknowledgments

Financial support for this study was provided by the U.S. Department of Energy (DOE) under Cooperative Agreement No. DE-FC01-06EW07053 entitled "Consortium For Risk Evaluation With Stakeholder Participation III." and by Colorado State University. The opinions, findings, conclusions, or recommendations expressed herein are those of the authors and do not necessarily

represent the views of the Department of Energy or Colorado State University.

References

- Albright, W., Benson, C., and Waugh, W. (2010). *Water balance covers for waste containment: Principles and practice*, ASCE, Reston VA, 158.
- Albright, W. H., et al. (2004). "Field water balance of landfill final covers." *J. Environ. Qual.*, 33(6), 2317–2332.
- Albright, W. H., Benson, C. H., and Apiwantragoon, P. (2013). "Field hydrology of landfill final covers with composite barrier layers." *J. Geotech. Geoenviron. Eng.*, 10.1061/(ASCE)GT.1943-5606.0000741, 1–12.
- Allen, R. G., Pereira, L. S., Raes, D., and Smith, M. (1998). "Crop evapotranspiration: Guidelines for computing crop requirements." *Irrigation and Drainage Paper No. 56*, Food and Agriculture Organization of the United Nations, Rome.
- Almorox, J. (2011). "Estimating global solar radiation from common meteorological data in Aranjuez, Spain." *Turk. J. Phys.*, 35(1), 53–64.
- Annandale, J. G., Jovanic, N. Z., Benade, N., and Allen, R. G. (2002). "Software for missing data error analysis Penman-Monteith reference evapotranspiration." *Irrig. Sci.*, 21(2), 57–67.
- Apiwantragoon, P., Benson, C., and Albright, W. (2014). "Field hydrology of water balance covers for waste containment." *J. Geotech. Geoenviron. Eng.*, 10.1061/(ASCE)GT.1943-5606.0001195, 04014101.
- ASTM. (2011). "Standard practice for classification of soils for engineering purposes (unified soil classification system)." *ASTM D2487*, West Conshohocken, PA.
- Benson, C. (2010). "Predictions in geoenvironmental engineering: Recommendations for reliable predictive modeling." *GeoFlorida 2010, advances in analysis, modeling, and design*, D. Fratta, A. Puppala, and B. Muhunthan, eds., ASCE, Reston, VA, 1–13.
- Benson, C. (2001). "Waste containment: Strategies and performance." *Aust. Geomech.*, 36(4), 1–25.
- Benson, C. (2007). "Modeling unsaturated flow and atmospheric interactions." *Theoretical and numerical unsaturated soil mechanics*, T. Schanz, ed., Springer, Berlin, 187–202.
- Benson, C. H., and Bareither, C. A. (2012). "Designing water balance covers for sustainable waste containment: Transitioning state-of-the-art to state-of-the-practice." *Geotechnical Engineering State of the Art and Practice: Keynote Lectures for GeoCongress 2012, GSP 226*, ASCE, Reston, VA, 1–33.
- Besharat, F., Dehghan, A. A., and Faghih, A. R. (2013). "Empirical models for estimating global solar radiation: A review and case study." *Renew. Sustainable Energy Rev.*, 21, 798–821.
- Böhm, W. (1979). *Methods of studying root systems*, Springer, New York.
- Bohnhoff, G., Ogorzalek, A., Benson, C., Shackelford, C., and Apiwantragoon, P. (2009). "Field data and water-balance predictions for a monolithic cover in a semiarid climate." *J. Geotech. Geoenviron. Eng.*, 10.1061/(ASCE)1090-0241(2009)135:3(333), 333–348.
- Campbell, G. S. (1985). *Soil physics with BASIC—Transport models for soil-plant systems*, Elsevier, New York.
- Campbell, G. S., and Norman, J. M. (1998). *An introduction to environmental biophysics*, 2nd Ed., Springer, New York.
- Doorenbos, J., and Pruitt, W. O. (1977). "Guidelines for predicting crop water requirements." *Irrigation and Drainage Paper 24*, Food and Agriculture Organization of the United Nations, Rome.
- Fayer, M., and Jones, T. (1990). "Unsaturated soil-water and heat flow model, ver. 2.0." Pacific Northwest Laboratory, Richland, WA.
- Fayer, M. J. (2000). "UNSAT-H version 3.0: Unsaturated soil water and heat flow model, theory, user manual, and examples." U.S. Dept. of Energy, Pacific Northwest National Laboratory, Richland, WA.
- Feddes, R., Kowalik, P., and Zaradny, H. (1978). *Simulation of field water use and crop yield*, Wiley, New York.
- Hargreaves, G. H. (1984). "Simplified coefficients for estimating monthly solar radiation in North America and Europe." Dept. Biological and Irrigation Engineering, Utah State Univ., Logan, UT.
- Hargreaves, G. H., and Samani, Z. A. (1982). "Estimating potential evapotranspiration." *J. Irrig. Drain. Div.*, 108(3), 225–230.
- Hubbard, K. G., Mahmood, R., and Carlson, C. (2003). "Estimating daily dew point temperature for the northern Great Plains using maximum and minimum temperature." *Agron. J.*, 95(2), 323–328.
- Khire, M., Benson, C., and Bosscher, P. (1997). "Water balance modeling of earthen final covers." *J. Geotech. Geoenviron. Eng.*, 10.1061/(ASCE)1090-0241(1997)123:8(744), 744–754.
- Khire, M., Benson, C., and Bosscher, P. (2000). "Capillary barriers: Design variables and water balance." *J. Geotech. Geoenviron. Eng.*, 10.1061/(ASCE)1090-0241(2000)126:8(695), 695–708.
- Khire, M. V., Benson, C. H., and Bosscher, P. J. (1999). "Field data from a capillary barrier and model predictions with UNSAT-H." *J. Geotech. Geoenviron. Eng.*, 10.1061/(ASCE)1090-0241(1999)125:6(518), 518–527.
- Kimball, J. S., Running, S. W., and Nemani, R. (1997). "An improved method for estimating surface humidity from daily minimum temperature." *Agric. Forest Meteorol.*, 85(1–2), 87–98.
- Malusis, M., and Benson, C. (2006). "Lysimeters versus water-content sensors for performance monitoring of alternative earthen final covers." *Unsaturated soils 2006*, Vol. 1, ASCE, Reston, VA, 741–752.
- Nyhan, J. W., Schofield, T. G., and Starmer, R. H. (1997). "A water balance study of four landfill cover designs varying in slope for semiarid regions." *J. Environ. Qual.*, 26(5), 1385–1392.
- Ogorzalek, A., Bohnhoff, G., Shackelford, C., Benson, C., and Apiwantragoon, P. (2007). "Comparison of field data and water-balance predictions for a capillary barrier cover." *J. Geotech. Geoenviron. Eng.*, 10.1061/(ASCE)1090-0241(2008)134:4(470), 470–486.
- Penman, H. L. (1948). "Natural evaporation from open water, bare soil and grass." *Proc. Roy. Soc. London*, A193, 120–146.
- Ritchie, J. T., and Burnett, E. (1971). "Dryland evaporative flux in a subhumid climate: II. Plant influences." *Agron. J.*, 63(1), 56–62.
- Roesler, A., Benson, C., and Albright, W. (2002). "Field hydrology and model predictions for final covers in the alternative cover assessment program." *Geo Engineering Rep. 02-08*, Univ. of Wisconsin-Madison, Madison, WI.
- Scanlon, B. R., Reedy, R. C., Keese, K. E., and Dwyer, S. F. (2005). "Evaluation of evapotranspirative covers for waste containment in arid and semiarid regions in the southwestern USA." *Vadose Zone J.*, 4(1), 55–71.
- Schaap, M. G., and Leij, F. J. (2000). "Improved prediction of unsaturated hydraulic conductivity with the Mualen-can Genuchten model." *Soil Sci. Soc. Am. J.*, 64(3), 843–851.
- Stormont, J., and Morris, C. (1998). "Method to estimate water storage capacity of capillary barriers." *J. Geotech. Geoenviron. Eng.*, 10.1061/(ASCE)1090-0241(1998)124:4(297), 297–302.
- Tallon, L. K., O'Kane, M. A., Chapman, D. E., Phillip, M. A., Shurniak, R. E., and Strunk, R. L. (2011). "Unsaturated sloping layered soil cover system: Field investigation." *Can. J. Soil Sci.*, 91(2), 161–168.
- van Genuchten, M. (1980). "A closed-form equation for predicting the hydraulic conductivity of unsaturated soils." *Soil Sci. Soc. Am. J.*, 44(5), 892–898.
- Wilcox, S. (2012). "National solar radiation database 1991-2010 update: User's manual." National Renewable Energy Laboratory, U.S. Dept. of Energy, Oak Ridge, TN.
- Zhang, W., and Sun, C. (2014). "Parametric analysis of evapotranspiration landfill covers in humid regions." *J. Rock Mech. Geotech. Eng.*, 6(4), 356–365.
- Zornberg, J. G., LaFountain, L., and Caldwell, J. A. (2003). "Analysis and design of evapotranspirative cover for hazardous waste landfill." *J. Geotech. Geoenviron. Eng.*, 10.1061/(ASCE)1090-0241(2003)129:6(427), 427–438.
- Zornberg, J. G., and McCartney, J. S. (2007). "Evapotranspirative cover systems for waste containment." *The handbook of groundwater engineering*, 2nd Ed., J. W. Delleur, ed., CRC Press, Boca Raton, FL, 34.1–34.31.